

MOLECULAR HYPERSTRUCTURES WITH HIGH SYMMETRY

Monica STEFU^{1,*}, Sorana D. BOLBOACA², Mugur BALAN¹, Lorentz JANTSCHI¹

¹Technical University of Cluj-Napoca, 103-105 Muncii Bvd., 400641 Cluj-Napoca. Romania.

²”Iuliu Hațieganu” University of Medicine and Pharmacy Cluj-Napoca, 6 Louis Pasteur, 400349 Cluj-Napoca, Romania. mstefu02@yahoo.com (* corresponding author)

Key words: map operations, C_{26} fullerenes, hyperstructures

Abstract: Starting from the structure of C_{26} fullerene and by using a series of map operations, a series of hyperstructures were obtained and investigated. A series of measures were performed in order to characterize the obtained hyperstructures and the estimations of the relationship between them were done. Images of two hyperstructures showing greatest informational entropy and lowest energy respectively between investigated ones, geometry optimized are given.

INTRODUCTION

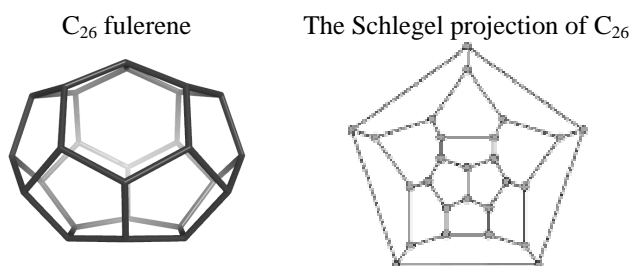
The Fullerenes are a family of carbon allotropes composed entirely of carbon of valence 3 (Kroto et al., 1985) and could be found in different forms as a hollow sphere, ellipsoid, tube or their derivations and combinations. A new research field of carbon-based materials with some extremely useful properties have been open since the discovery of fullerene buckyballs (the most known, C_{60} , was discovered in 1985, by Richard Buckminster Fuller), and carbon nanotubes (Sumio, 1991). Since their discovery, a series of properties have been identified and studied: aggregation (Zhang et al., 2008; Wong-Ekkabut et al., 2008), vibrational (Graja et al., 2008), antibiofouling potential (Lyon et al., 2008), cytotoxicity and antibacterial properties (Lyon et al., 2008), photoabsorption (Koponen et al., 2008), emission and magneto-optic properties (Noiseux et al., 2008), etc.

A series of map operations (Diudea, 2005; Diudea, 2004; Klein et al., 1997) have been introduced and proved their abilities in generation of theoretical models of fullerenes with various size faces and coverings (Ștefu and Diudea, 2007). In presented research the map operations (Ștefu and Diudea, 2007) were used for generating hyper-structures starting from an isomer of C_{26} fullerene. The obtained hyperstructures were characterized by using a series of parameters and the links between them were investigated.

MATERIAL AND METHOD

An isomer of the the C_{26} fullerene (Figure 1) was the starting structure from which the hyperstructures were obtained.

A graph is *embedded* in a surface S when it is drawn on S in that manner in which any two edges do not intersect each other (Harary, 1969). A graph is planar if it can be embedded in a plane. A *map* M is a combinatorial representation of a graph embedded in a surface (Pisanski and Randić, 2000) and creates a tessellation on that surface. The *map operations* are geometrical and topological transformations of a given map. The following notations are used in a map: v - the number of vertices, e - the number of edges, f - the number of faces. For example, the C_{26} fullerene has all vertices of degree 3, $v_3 = 26$, $e = 39$ and 15 faces from which of size 5 and 6 ($f_5 = 12$, and $f_6 = 3$, respectively).



An isomer of the C_{26} fullerene

Figure 1.

The *Map Operations* can be classified in simple, composite, generalized and other operations (Diudea and John, 2001; Diudea, 2004; Diudea, 2005). The simple and composite operations used in this study were implemented into a computer program (CVNET; Ştefu and Diudea, 2007) which was used in construction of hyper-structures based on structure of fullerene C_{26} . The summary of these operations is presented in Table 1.

Table 1.

Map Operations			
Type	Name	Description	Ref
Simple			
1	<i>Dualization (Du)</i>	<i>Du</i> of a map locate new a point in the centre of each face and join two such points if their corresponding faces share a common edge.	(Pisanski and Randić, 2000)
2	<i>Medial (Me)</i>	<i>Me</i> puts the new vertices as the midpoints of the original edges and join two vertices if and only if the original edges are incident and consecutive on a face in the original map.	(Fowler and Pisanski, 1994)
3	<i>Truncation (Tr)</i>	<i>Tr</i> puts two new vertices on each edge, then for each old vertex joins the new vertices around them, finally cut off the old vertex.	(Pisanski and Randić, 2000)
4	<i>Stellation (St)</i>	<i>St</i> adds a new vertex in the center of every face and connects it with the boundary vertices. The old vertices and edges are kept.	(Pisanski and Randić, 2000)
5	<i>Capping (P₄)</i>	<i>P₄</i> adds a new vertex in the center of every face and puts new vertices as the midpoints of the original edges. Connect the new vertices from every face center with the edges midpoints of that face.	(Diudea, 2004)
6	<i>P₅</i>	<i>P₅</i> adds a new vertex in the center of every face and puts two new vertices on each edge. For every face, connects then the vertices from the face centre alternatively with the vertices from the edges.	(Diudea, 2004)
Composite			
1	<i>Leapfrog Le</i>	$Le = Du \cdot St = Tr \cdot Du$	(Diudea et al., 2003)
2	<i>Quadrupling Q</i>	<i>Q</i> adds a new cycle of the same size inside of each cycle/face and connects the two cycles vertex by vertex. Next, the old edges are deleted. The transformation preserves the initial orientation of all parent faces in the map as well as the initial vertices	(Fowler et al., 1988)
3	<i>Capra Ca</i>	<i>Ca</i> puts two new points on each edge of the map. Next, puts a new cycle of the same size in the center of each face and connects the vertices from the face centre alternatively with the vertices from the edges.	(Diudea, 2003; Diudea, 2005)

Note: *Capra* and *P₅* are chiral operations (have two variants) and generate chiral objects

A series of QSAR (Quantitative Structure-Activity Relationships) parameters were calculated on the obtained hyperstructures by using HyperChem (HyperChem, 2008): volume (Vol), hydration energy (HydE), logarithm of octanol (LogP), refractivity index (Ref), and polarizability index (Pol). In addition, informational entropy (Ent) and energy (Eng) of the faces were calculated starting from the following knowledge:

÷ The number of total faces are known

- ÷ The size of faces are known (see Table 2)
- ÷ The probabilities (abbreviated as p) associated to the occurrence of a face of a given size (event x_i below) can be obtained and were used to obtain the informational entropy (Shannon, 1948) and energy (Onicescu, 1966) of the resulted structure:

$$\text{Ent} = -\sum_{i=1}^p p(x_i) \log_2(p(x_i)) \text{ and } \text{Eng} = \sum_{i=1}^n p^2(x_i)$$

The link analysis was performed by computing a series of correlation coefficients and associated probabilities (Bolboacă and Jäntschi, 2006; Bolboacă et al., 2008).

RESULTS

Starting from the C_{26} fullerene (Figure 1), a series of map operations were performed and the characteristics of the resulted hyperstructures are presented in Table 2.

Table 2.

QSAR parameters on resulted structure on investigated C_{26} fullerene

Op.	V	E	Faces (total- f_i ; and by size - f_i)	Ent	Eng	Vol	HydE	LogP	Ref	Pol
Du*	15	39	$f=26; f_3=26$	0.000	1.000	417.3	0.00	0.00	0.00	0.00
Me	39	78	$f=41; f_3=26; f_5=12; f_6=3$	0.885	0.493	763.3	0.00	-5.33	102.20	41.38
Tr	78	117	$f=41; f_3=26; f_{10}=12; f_{12}=3$	0.885	0.493	1785.0	-0.78	0.00	0.00	105.50
St*	41	117	$f=78; f_3=78$	0.000	1.000	701.66	0.00	0.00	0.00	0.00
P ₄ *	80	156	$f=78; f_4=78$	0.000	1.000	1413.33	-0.12	-5.33	102.20	960.88
P ₅ *	119	195	$f=78; f_5=78$	0.000	1.000	1803.5	-0.16	0.00	0.00	140.61
Le	78	117	$f=41; f_3=12; f_6=29$	1.773	0.586	1556.0	-0.49	0.00	0.00	105.50
Q	104	156	$f=54; f_3=12; f_6=42$	2.170	0.654	2001.0	-0.62	0.00	0.00	140.60
Ca	182	273	$f=93; f_3=12; f_6=81$	2.954	0.775	3350.0	-1.01	-0.46	7.88	246.10
Le·Q	312	468	$f=158; f_3=12; f_6=146$	3.719	0.86	5600.7	-1.67	0.00	0.00	421.80
Le·Ca	546	819	$f=275; f_3=12; f_6=263$	4.518	0.917	8831.3	-1.91	0.00	0.00	738.20
Q·Ca	728	1092	$f=366; f_3=12; f_6=354$	4.931	0.937	12801.0	-3.82	0.00	0.00	984.20
Le·Le	234	351	$f=119; f_3=12; f_6=107$	3.310	0.819	3915.27	-0.85	0.00	0.00	316.37
Q·Q	416	624	$f=210; f_3=12; f_6=198$	4.129	0.892	6767.85	-1.46	0.00	0.00	562.43
Du·Le	78	117	$f=41; f_3=26; f_{10}=12; f_{12}=3$	0.885	0.493	1446.9	-0.43	0.00	0.00	105.46
Le·Du*	41	117	$f=78; f_3=78$	0.000	1.000	701.5	0.00	0.00	0.00	0.00
Du·Q*	93	156	$f=65; f_3=26; f_6=39;$	1.322	0.520	1746.3	-0.28	0.00	0.00	105.46
Q·Du*	54	156	$f=104; f_3=104;$	0.000	1.000	914.92	0.00	0.00	0.00	0.00
Du·Ca*	171	273	$f=104; f_3=26; f_6=78;$	2.000	0.625	2992.2	-0.34	0.00	0.00	210.91
Ca·Du*	93	273	$f=182; f_3=182;$	0.000	1.000	1275.8	0.00	0.00	0.00	0.00
Tr·Le	234	351	$f=119; f_3=26; f_6=78; f_{10}=12; f_{12}=3;$	2.385	0.488	3885.8	-0.50	0.00	0.00	316.37
Tr·Q	312	468	$f=158; f_3=26; f_6=117; f_{10}=12; f_{12}=3;$	2.747	0.582	5528.1	-1.15	0.00	0.00	421.82
Tr·Ca	546	819	$f=275; f_3=26; f_6=234; f_{10}=12; f_{12}=3;$	3.486	0.735	8473.9	-1.89	0.00	0.00	738.19
Ca·Med	273	546	$f=275; f_3=182; f_5=12; f_6=81;$	0.940	0.527	3898.67	0.00	-37.29	715.40	289.85
Ca·Tr	546	819	$f=275; f_3=182; f_{10}=12; f_{12}=81;$	0.940	0.527	7992.91	-0.59	0.00	0.00	738.19
Le·Med	117	234	$f=119; f_3=78; f_5=12; f_6=29;$	0.957	0.499	1794.90	0.00	-15.98	306.60	124.14
Le·Tr	234	351	$f=119; f_3=78; f_{10}=12; f_{12}=29;$	0.957	0.499	3714.92	-0.46	0.00	0.00	316.37
Q·Med	156	312	$f=158; f_3=104; f_5=12; f_6=42;$	0.951	0.510	2324.97	0.00	-21.31	408.80	165.52
Q·Tr	312	468	$f=158; f_3=104; f_{10}=12; f_{12}=42;$	0.951	0.510	6459.84	-1.81	0.00	0.00	421.82
P ₅ ·Ca*	899	1365	$f=468; f_3=78; f_6=390;$	2.585	0.722	13145.51	-1.35	0.00	0.00	1195.17
P ₅ ·Le*	390	585	$f=197; f_3=78; f_6=104; f_{10}=12; f_{12}=3;$	1.573	0.439	6660.22	-1.36	0.00	0.00	527.28
P ₅ ·Q*	509	780	$f=273; f_3=78; f_6=195;$	1.807	0.592	7400.17	-0.78	0.00	0.00	667.89

Op = operation(s) on C_{26} ; V = number of vertices; E = number of edges; Ent = entropy; Eng = energy; Vol = molecular volume (\AA^3);

HydE = hydration energy (kcal/mol); LogP = log. of octanol/water partition coefficient (a-dimensional); Ref = refractivity index (\AA^3); Pol = polarizability index (\AA^3);

*: produces a structure with vertex degree larger than 4

DISCUSSIONS

The resulted characteristics of the hyperstructures were analyzed using correlation matrix presented in Table 3.

Two properties, represented by logarithm of octanol/water partition coefficient and refractivity index were not included in correlation analysis due to the impossibility of HyperChem to calculate reliable values.

The following remarks can be stated by analyzing the correlation coefficients:

- ÷ The methods used in calculating the correlation coefficients shows that the results were not always concordant (e.g. if one correlation coefficient was statistically significant all others has to be also statistically significant to be considered as true correlation). Following are exceptions: entropy – total number of faces (Γ not significant); hydration energy – volume (not significant Kendall's correlation coefficients); hydration energy – polarizability index (not significant τ_a , τ_b , and τ_c), etc. These discordances can be explained by the complexity of hyperstructures, the HyperChem was not able to compute the QSAR parameters (see the value from Table 2).
- ÷ Good correlations (statistically significant) were found between five characteristics: the number of vertices (V), number of edges (E), number of faces (F), informational entropy, volume and polarizability (with exception between volume – the number of faces, and between volume – polarizability, where τ_a , τ_b , τ_c and Γ are not significant). There was expected to obtained a good correlation coefficients between V, F and E due to link between them gave by the the Euler formulas $\sum dv_d = \sum sf_s = 2e$ (Euler, 1736)

where d = vertex degree, v_d = valence of vertex v , e = number of edges, s = face size, f_s = size of face f). There were also expected to found good and significant correlations between V, E, F and hyperstructure volume. Weak to moderate correlations were identified between informational entropy and number of vertices and number of edges, respectively. The absence of informational entropy has been identified for the hyperstructures in which the structure has just one faces size.

The optimized structure of the hyperstructures with highest entropy ($Q\cdot Ca(C_{26})$) and the one with lowest energy ($P_5\cdot Le(C_{26})$) are graphically represented in Figure 2.

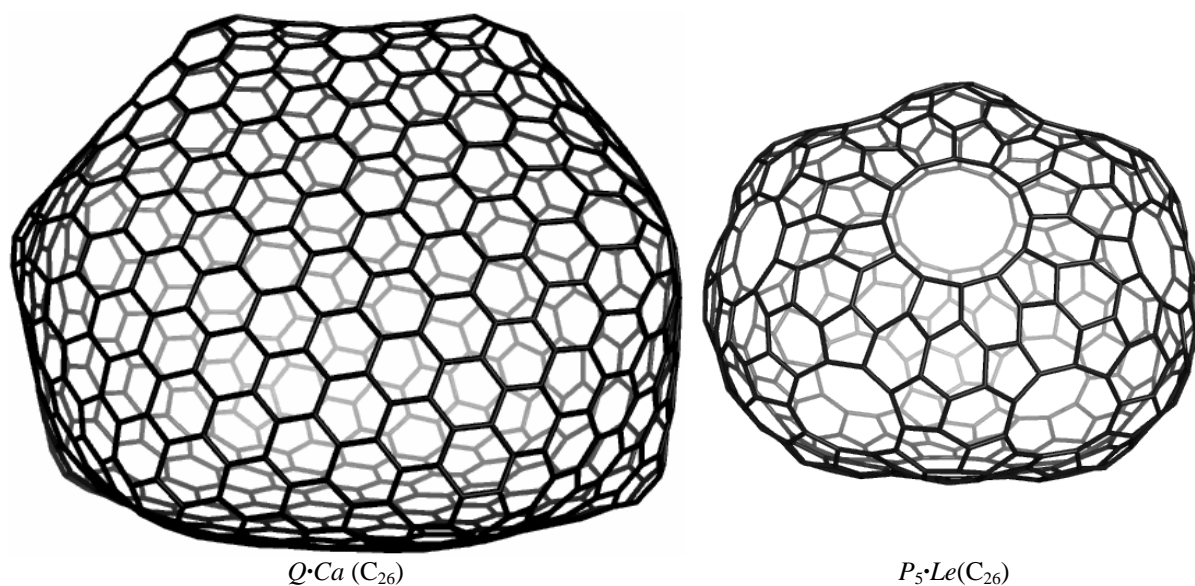


Figure 2.
Representation of hyperstructures with highest entropy ($Q\cdot Ca(C_{26})$) and lowest energy ($P_5\cdot Le(C_{26})$)

Table 3.

Correlation matrix on hyperstructures

	E	F	Ent	Eng	Vol	HydE	Pol	
V (number of vertices)	r	0.99(3.6·10 ⁻³⁰)	0.94(1.3·10 ⁻¹⁵)	0.66(4.1·10 ⁻⁵)	-0.05(0.79)	0.99(6.1·10 ⁻²⁷)	-0.75(9.2·10 ⁻⁷)	0.88(4.6·10 ⁻¹¹)
	S _Q	0.99(3.0·10 ⁻²⁶)	0.92(1.8·10 ⁻¹³)	0.70(9.8·10 ⁻⁶)	0.07(0.69)	0.99(2.9·10 ⁻²⁶)	0.75(8.1·10 ⁻⁷)	0.89(1.7·10 ⁻¹¹)
	ρ	0.98(7.7·10 ⁻²⁴)	0.89(6.3·10 ⁻¹²)	0.73(1.7·10 ⁻⁶)	-0.11(0.53)	0.99(1.2·10 ⁻²⁵)	-0.75(7.1·10 ⁻⁷)	0.89(6.1·10 ⁻¹²)
	τ _a	0.89(6.8·10 ⁻¹³)	0.74(2.4·10 ⁻⁹)	0.53(1.7·10 ⁻⁵)	0.039(0.80)	0.92(1.4·10 ⁻¹³)	0.56(0.99)	0.81(5.7·10 ⁻¹¹)
	τ _b	0.89(6.8·10 ⁻¹³)	0.74(2.4·10 ⁻⁹)	0.55(1.5·10 ⁻⁵)	0.039(0.80)	0.92(1.4·10 ⁻¹³)	0.57(0.99)	0.82(5.2·10 ⁻¹¹)
	τ _c	0.87(3.4·10 ⁻¹²)	0.72(7.4·10 ⁻⁹)	0.52(2.8·10 ⁻⁵)	0.04(0.77)	0.89(7.9·10 ⁻¹³)	0.54(0.99)	0.79(2.0·10 ⁻¹⁰)
	Γ	0.95(4.6·10 ⁻¹³)	0.79(4.2·10 ⁻⁷)	0.58(6.8·10 ⁻³)	0.04(0.99)	0.95(6.1·10 ⁻¹³)	0.61(2.9·10 ⁻³)	0.86(3.8·10 ⁻⁹)
E (number of edges)	r	1	0.97(1.6·10 ⁻²⁰)	0.62(1.6·10 ⁻⁴)	-0.02(0.89)	0.98(1.5·10 ⁻²¹)	-0.71(5.7·10 ⁻⁶)	0.86(2.0·10 ⁻¹⁰)
	S _Q	1	0.96(8.1·10 ⁻¹⁹)	0.64(7.2·10 ⁻⁵)	0.04(0.85)	0.97(4.1·10 ⁻¹⁹)	0.69(1.4·10 ⁻⁵)	0.86(2.5·10 ⁻¹⁰)
	ρ	1	0.96(1.7·10 ⁻¹⁷)	0.67(2.9·10 ⁻⁵)	-0.05(0.78)	0.95(2.3·10 ⁻¹⁷)	-0.67(3.2·10 ⁻⁵)	0.86(3.2·10 ⁻¹⁰)
	τ _a	1	0.82(3.7·10 ⁻¹¹)	0.47(1.7·10 ⁻⁴)	0.01(0.05)	0.84(1.5·10 ⁻¹¹)	0.48(0.99)	0.74(2.4·10 ⁻⁹)
	τ _b	1	0.82(3.7·10 ⁻¹¹)	0.49(1.5·10 ⁻⁴)	0.01(0.05)	0.84(1.5·10 ⁻¹¹)	0.50(0.99)	0.75(2.2·10 ⁻⁹)
	τ _c	1	0.80(1.5·10 ⁻¹⁰)	0.45(2.5·10 ⁻⁴)	0.01(0.05)	0.81(6.4·10 ⁻¹¹)	0.46(0.99)	0.72(6.9·10 ⁻⁹)
	Γ	1	0.91(3.8·10 ⁻¹¹)	0.52(0.03)	0.01(0.99)	0.89(2.0·10 ⁻¹⁰)	0.54(0.02)	0.80(2.0·10 ⁻⁷)
F (number of faces)	r		1	0.51(2.9·10 ⁻³)	0.02(0.89)	0.91(6.2·10 ⁻¹³)	-0.60(2.9·10 ⁻⁴)	0.80(3.9·10 ⁻⁸)
	S _Q		1	0.51(2.7·10 ⁻³)	0.03(0.86)	0.87(6.5·10 ⁻¹¹)	0.54(1.5·10 ⁻³)	0.77(2.7·10 ⁻⁷)
	ρ		1	0.52(2.5·10 ⁻³)	0.04(0.81)	0.84(1.8·10 ⁻⁹)	-0.48(5.0·10 ⁻³)	0.74(1.4·10 ⁻⁶)
	τ _a		1	0.34(5.8·10 ⁻³)	0.044(0.72)	0.69(3.2·10 ⁻⁸)	0.33(0.99)	0.60(1.2·10 ⁻⁶)
	τ _b		1	0.35(5.6·10 ⁻³)	0.045(0.72)	0.69(3.2·10 ⁻⁸)	0.34(0.99)	0.61(1.2·10 ⁻⁶)
	τ _c		1	0.33(7.2·10 ⁻³)	0.043(0.73)	0.67(8.5·10 ⁻⁸)	0.32(0.99)	0.58(2.5·10 ⁻⁶)
	Γ		1	0.38(0.25)	0.05(0.98)	0.73(1.5·10 ⁻⁵)	0.38(0.25)	0.66(5.1·10 ⁻⁴)
Ent (Entropy)	r			1	0.01(0.96)	0.71(6.1·10 ⁻⁶)	-0.81(1.9·10 ⁻⁸)	0.55(1.0·10 ⁻³)
	S _Q			1	0.035(0.85)	0.74(1.2·10 ⁻⁶)	0.80(2.8·10 ⁻⁸)	0.60(2.9·10 ⁻⁴)
	ρ			1	-0.13(0.49)	0.78(1.7·10 ⁻⁷)	-0.80(4.1·10 ⁻⁸)	0.65(6.1·10 ⁻⁵)
	τ _a			1	0.06(0.64)	0.59(2.4·10 ⁻⁶)	0.60(0.99)	0.50(5.0·10 ⁻⁵)
	τ _b			1	0.06(0.639)	0.60(2.0·10 ⁻⁶)	0.63(0.99)	0.52(4.4·10 ⁻⁵)
	τ _c			1	0.06(0.64)	0.57(4.2·10 ⁻⁶)	0.58(0.99)	0.49(7.5·10 ⁻⁵)
	Γ			1	0.06(0.97)	0.62(1.9·10 ⁻³)	0.66(4.2·10 ⁻⁴)	0.54(0.02)
Eng (Energy)	r				1	-0.05(0.79)	-0.07(0.71)	0.05(0.815)
	S _Q				1	0.09(0.61)	0.08(0.68)	0.06(0.74)
	ρ				1	-0.18(0.33)	0.08(0.64)	-0.08(0.66)
	τ _a				1	0.07(0.43)	0.02(0.90)	0.01(0.03)
	τ _b				1	0.07(0.43)	0.02(0.89)	0.01(0.03)
	τ _c				1	0.068(0.42)	0.02(0.89)	0.00(0.02)
	Γ				1	0.07(0.97)	0.02(0.99)	0.01(0.99)
Vol (Volume)	r					1	-0.83(5.4·10 ⁻⁹)	0.87(8.3·10 ⁻¹¹)
	S _Q					1	0.82(1.3·10 ⁻⁸)	0.88(2.8·10 ⁻¹¹)
	ρ					1	-0.80(2.9·10 ⁻⁸)	0.89(8.6·10 ⁻¹²)
	τ _a					1	0.63(0.99)	0.84(1.1·10 ⁻¹¹)
	τ _b					1	0.64(0.99)	0.85(9.8·10 ⁻¹²)
	τ _c					1	0.60(0.99)	0.82(4.2·10 ⁻¹¹)
	Γ					1	0.67(3.6·10 ⁻⁴)	0.87(7.5·10 ⁻¹⁰)
HydE (hydration)	r						1	-0.67(3.1·10 ⁻⁵)
	S _Q						1	0.70(8.3·10 ⁻⁶)
	ρ						1	-0.73(1.7·10 ⁻⁶)
	τ _a						1	0.55(0.99)
	τ _b						1	0.57(0.99)
	τ _c						1	0.53(0.99)
	Γ						1	0.60(4.3·10 ⁻³)

CONCLUSIONS

A number of 32 structures obtained by map operations on C₂₆ fullerene were considered, and for each, ten parameters were calculated: the number of vertices, edges and faces, informational entropy and energy, volume, hydration energy, and polarizability index.

A good correlation was found between the number of vertices, faces, edges, volume and polarizability. Informational entropy and informational energy, calculated on the basis of the faces sizes, were moderate/low correlated (entropy) or not correlated (energy) with the other investigated characteristics. Because at the most of structures, the LogP and the Ref index could not be calculated, these parameters were not considered in correlation analysis.

REFERENCES

1. Bolboacă SD, EM Pică, CV Cimpoiu, L Jäntschi, 2008, Statistical Assessment of Solvent Mixture Models Used for Separation of Biological Active Compounds, *Molecules*, 8(13), 1617-1639.
2. Bolboacă SD, L Jäntschi, 2006, Pearson Versus Spearman, Kendall's Tau Correlation Analysis on Structure-Activity Relationships of Biologic Active Compounds, *Leonardo J Sci*, 9, 179-200.
3. Diudea M. V., and P. E. John, 2001, Covering polyhedral tori. *Commun. Math. Comput. Chem. (MATCH)*, 44 103-116.
4. Diudea MV, 2004, Covering Forms in Nanostructures, *Forma (Tokyo)*, 19(3), 131-163.
5. Diudea MV, 2005, Covering Nanostructures, In: M. V. Diudea (Ed.), *Nanostructures-Novel Architecture*, NOVA, New York, pp. 203-242.
6. Diudea MV, PE John, A Graovac, M Primorac, T Pisanski, 2003, Leapfrog and Related Operations on Toroidal Fullerenes. *Croat. Chem. Acta*, 76, 153-159.
7. Euler L., 1736, *Comment. Acad. Sci. I. Petropolitanae* 8,128-140.
8. Fowler PW, JE Cremona, JI Steer, 1988, Systematics of bonding in non-icosahedral carbon clusters, *Theor. Chim. Acta*, 73(1), 1-26.
9. Fowler PW, T Pisanski, 1994, Leapfrog Transformation and polyhedra of Clar Type, *J. Chem. Soc. Faraday Trans.*, 90, 2865-2871.
10. Graja A, K Lewandowska, B Laskowska, A Łapiński, D Wróbel, 2008, Vibrational properties of thin films and solid state of perylenediimide-fullerene dyads, *Chemical Physics*, In press.
11. Harary F, 1969, *Graph Theory*, Addison - Wesley, Reading, M.A.
12. HyperChem, 2008, URL: <http://www.hyper.com/>
13. Klein D. J., Zhu H., 1997, in: A. T. Balaban, (Ed.), *From Chemical Topology to Three - Dimensional Geometry*, Plenum Press, New York, pp. 297-341.
14. Koponen L, MJ Puska, RM Nieminen, 2008, Photoabsorption spectra of small fullerenes and Si-heterofullerenes, *Journal of Chemical Physics*, 128(15), 154307 (article number).
15. Kroto HW, JR Heath, SC O'Brien, RF Curl, RE Smalley, 1985, C₆₀: Buckminsterfullerene. *Nature* 318, 162-163.
16. Lyon DY, D Brown, ER Sundstrom, PJJ Alvarez, 2008, Assessing the antibiofouling potential of a fullerene-coated surface, *International Biodeterioration Biodegradation*, In press.
17. Lyon DY, L Brunet, GW Hinkal, MR Wiesner, PJ Alvarez, 2008, Antibacterial activity of fullerene water suspensions (nC₆₀) is not due to ROS-mediated damage, *Nano letters*, 8(5), 1539-1543.
18. Mermut O, J-P Bouchard, J-F Cormier, P Desroches, KR Diamond, M Fortin, P Gallant, S Leclair, J-S Marois, I Noiseux, J-F Morin, MS Patterson, M Vernon, 2008, Time-resolved luminescence measurements of the magnetic field effect on paramagnetic photosensitizers in photodynamic reactions, *Progress in Biomedical Optics and Imaging - Proceedings of SPIE*, 6845, 68450T (article number).
19. Onicescu O, 1966, *Energie informationelle*, *Compt. Rend. Acad. Sci. Paris Ser. A*, 263, 841-841.
20. Pisanski T, M Randić, 2000, *Geometry at Work*, M. A. A. Notes, 53, 174-194.
21. Shannon CE, 1948, *A Mathematical Theory of Communication*, *Bell. Syst. Techn. J.*, 27, 379-423, 623-656.
22. Ștefu M, MV Diudea, 2007, *CageVersatile (.Net)*, "Babes-Bolyai" University, Cluj (computer program).
23. Sumio I, 1991, Helical microtubules of graphitic carbon, *Nature*, 354, 56-58.
24. Wong-Ekkabut J, S Baoukina, W Triampo, I-M Tang, DP Tieleman, L Monticelli, 2008, Computer simulation study of fullerene translocation through lipid membranes, *Nature Nanotechnology*, 3(6), 363-368.
25. Zhang P, ZX Guo, S Lv, 2008, Synthesis and aggregation properties of amphiphilic mono and bisadducts of fullerene in aqueous solution, *Chinese Chemical Letters*, 19(9), 1039-1042.